THE JOURNAL OF PHYSICAL CHEMISTRY Letters

Letter

Cite This: J. Phys. Chem. Lett. 2019, 10, 164−170

pubs.acs.org/JPCL

Origin of Anisotropic Molecular Packing in Vapor-Deposited Alq3 Glasses

Kushal Bagchi,[†] Nicholas E. Jackson,[‡,§] Ankit Gujral,[†] Chengbin Huang,[∥] Michael F. Toney,[⊥] Lian Yu,[∥] Juan J. de Pablo,[‡,§] and M. D. Ediger*[,†]

[†]Department of Chemistry, University of Wisconsin—Madison, Madison, Wisconsin 53706, United States

[‡]Institute for Molecular Engineering, University of Chicago, Chicago, Illinois 60637, United States

[§]Institute for Molecular Engineering, Argonne National Laboratory, Lemont, Illinois 60439, United States

[∥]School of Pharmacy, University of Wisconsin—Madison, 777 Highland Avenue, Madison, Wisconsin 53705-2222, United States

[⊥]Stanford Synchrotron Radiation Lightsource, SLAC National Accelerator Laboratory, Menlo Park, California 94025, United States

Supporting Information

ABSTRACT: Anisotropic molecular packing is a key feature that makes glasses prepared by physical vapor deposition (PVD) unique materials, warranting a mechanistic understanding of how a PVD glass attains its structure. To this end, we use X-ray scattering and ellipsometry to characterize the structure of PVD glasses of tris(8-hydroxyquinoline) aluminum (Alq3), a molecule used in organic electronics, and compare our results to simulations of its supercooled liquid. X-ray scattering reveals a tendency for molecular layering in Alq3 glasses that depends upon the substrate temperature during deposition and the deposition rate. Simulations reveal that the Alq3 supercooled liquid, like liquid metals, exhibits surface layering. We propose that the layering in Alq3 glasses observed here as well as the previously reported bulk dipole orientation are inherited from the surface structure of the supercooled liquid. This work significantly advances our understanding of the mechanism governing the formation of anisotropic structure in PVD glasses.

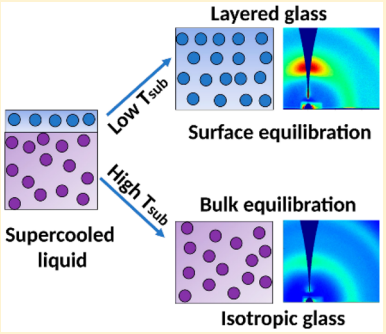

Vapor-deposited glasses have attracted wide interest in recent years for use in organic electronics[1,2] and as a means to advance glass science.[3] Vapor-deposited organic glasses are interesting from a fundamental viewpoint for several reasons. When prepared at the optimal substrate temperature and deposition rate, PVD glasses have properties expected for liquid-cooled glasses that have been annealed for thousands of years such as higher density[4] and lower enthalpy.[5] Vapor-deposited glasses illustrate how the properties of amorphous materials evolve on reaching lower positions in the potential energy landscape[6,7] and therefore help us understand the "ultimate properties" of amorphous materials. The efficient packing of these materials reduces residual molecular mobility in the glassy state, as exhibited by suppression of both secondary relaxation processes[8] and quantum mechanical tunneling systems that become prominent in glasses near T = 0 K.[9] For technological applications in organic electronics, vapor-deposited glasses are attractive, as they have been shown to exhibit superior physical and chemical properties such as greater photostability[10] and lower uptake of atmospheric gases,[11] as compared to their liquid-cooled counterparts. For organic semiconductors, the substrate temperature during deposition of a PVD glass can be chosen to maximize charge transport by optimizing orbital overlap between adjacent molecules.[12]

PVD harnesses the enhanced mobility at the free surface of an organic glass to produce important and useful properties such as high density; surface mobility can be many orders of magnitude larger than bulk mobility.[13,14] As each molecule is at some point at the vacuum interface, it can partially equilibrate with its neighbors before being buried by subsequent deposition, even though the temperature is below the glass transition temperature T_g. This process enables molecules to sample configurational space with high efficiency, and this leads to favorable local packing arrangements and high density. Vapor-deposited glasses retain the advantageous properties of conventional glasses such as compositional flexibility and macroscopic homogeneity (lack of grain boundaries); these two factors are important reasons why the charge transport and emitter layers in commercial organic light-emitting diodes (OLEDs) are vapor-deposited glasses as opposed to crystals.

In contrast to liquid-cooled glasses, PVD glasses can be anisotropic[1,15,16] and this is technologically relevant for device performance.[17,18] For example, in-plane molecular orientation of the transition dipoles of emitter molecules has been shown to be advantageous for light outcoupling efficiency in OLEDs.[1,19] This orientational anisotropy is characterized

Received: November 28, 2018
Accepted: December 24, 2018
Published: December 24, 2018

DOI: 10.1021/acs.jpclett.8b03582
J. Phys. Chem. Lett. 2019, 10, 164−170

through the average value of the second Legendre polynomial (P_2) for the transition dipole. P_2 order is observed experimentally through the orientation-dependent emission intensity[20] and through UV,[21] IR,[22] or soft X-ray dichroism.[23] The extent of P_2 order in PVD glasses can be controlled by varying the substrate temperature during deposition.[4] On the basis of molecular dynamics simulations of the supercooled liquid state of three organic semiconductors, it has been proposed that the P_2 anisotropy observed experimentally in the bulk of vapor-deposited glasses is inherited from orientational anisotropy at the free surface of the equilibrium supercooled liquid.[4,24] This mechanism by which a PVD glass acquires its high density and P_2 order has been called the "surface equilibration mechanism".

In addition to P_2 order, PVD glasses are structurally anisotropic in two other respects. Vapor-deposited glasses often show a broad anisotropic peak in X-ray scattering patterns at a real space distance roughly corresponding to a molecular diameter.[25,26] The underlying modulation in the electron density along the surface normal can be interpreted as a tendency for center of mass ordering,[27] and we refer to this below as "molecular layering". In contrast to the P_2 orientational order discussed above, the anisotropic scattering feature associated with layering is a result of translational order. For polymeric semiconductors,[28] similar anisotropic scattering features are associated with high charge mobility and this may also be true for molecular semiconductors. Despite molecular layering being a common feature of vapor-deposited glasses, both its origin and its relation to function are unexplored. Vapor-deposited glasses are also known to exhibit spontaneous polarization.[29,30] This feature arises due to preferential orientation of the dipole moment vector in the bulk of the film and is known to influence charge injection in organic electronics devices.[31] In contrast to P_2 order, our understanding of how substrate temperature and deposition rate influence these additional anisotropic features is much less advanced. We emphasize that anisotropic X-ray scattering and spontaneous polarization cannot be predicted from a measurement of P_2 order. Vapor deposition of some molecules results in glasses with spontaneous polarization but no P_2 order,[30] while, for other molecules, glasses can be prepared that exhibit anisotropic scattering[32] without P_2 order or spontaneous polarization. It remains to be seen if all of the different aspects of anisotropic structure in a PVD glass can be explained within one unifying "umbrella" mechanism.[33] Such a mechanism would be broadly applicable to PVD glasses of all types of molecules. In this Letter, we test if the surface equilibration mechanism serves as such a unifying mechanism.

In this study, we characterize the structure of vapor-deposited glasses of the common OLED molecule Alq3 with grazing incidence wide-angle X-ray scattering (GIWAXS) and spectroscopic ellipsometry. We also perform molecular dynamics simulations of the supercooled liquid of Alq3. As we find here that vapor-deposited glasses of Alq3 exhibit a tendency for molecular layering, this is a good system for testing if the surface equilibration mechanism can account for the anisotropic X-ray scattering associated with this feature. We find that the tendency for molecular layering in vapor-deposited Alq3 glasses depends upon the substrate temperature during deposition; these same glasses are nearly optically isotropic. Despite being extensively used in OLED devices, anisotropic scattering in Alq3 glasses has not been previously reported. Interestingly, simulations reveal that supercooled Alq3, like liquid metals such as gallium,[34] exhibits surface layering. These simulation studies of the surface of the supercooled liquid of Alq3 show that molecular layering, measured for Alq3 for the first time, can be explained by the surface equilibration mechanism.

An additional test of the surface equilibration mechanism was performed using the simulations reported here. It has been long known that PVD glasses in general (and Alq3 glasses, in particular) can exhibit "spontaneous polarization".[29,30] For depositions onto substrates at room temperature, for example, this manifests as a surface potential that grows by a constant 40 mV for every nanometer of Alq3 deposited. This spontaneous polarization therefore arises from a tendency for dipole orientation in the bulk of the PVD glass.[29] The direction of dipole orientation determines if the surface potential is positive or negative and influences charge injection barriers in devices.[31] The simulations of the supercooled Alq3 liquid, in combination with the surface equilibration mechanism, correctly account for the sign of the surface potential of Alq3 glasses. This result both suggests a means of generally predicting the sign of the surface potential and provides an important confirmation of the validity of the surface equilibration mechanism.

Shown in Figure 1 are the GIWAXS patterns from glasses of Alq3 vapor-deposited onto silicon substrates held at different

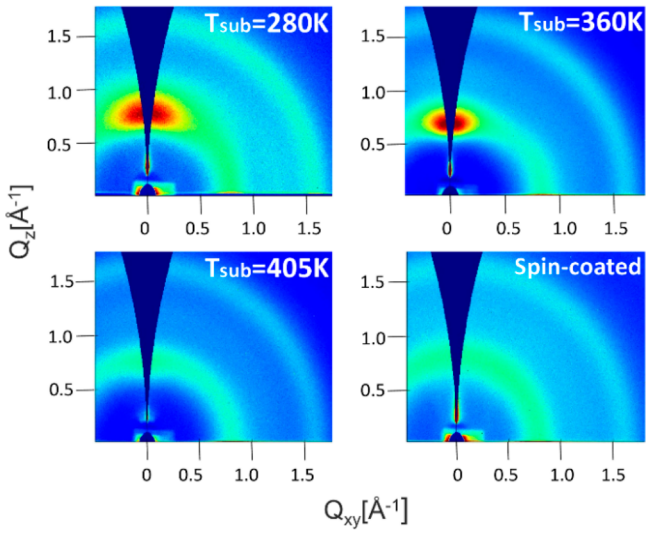

Figure 1. GIWAXS patterns for Alq3 glasses prepared at T_{sub} = 280 K, T_{sub} = 360 K, and T_{sub} = 405 K and a reference spin-coated glass. An anisotropic scattering feature related to molecular layering is prominently observed for the two lowest substrate temperatures. Q_z is the out-of-plane scattering vector, and Q_{xy} is the in-plane scattering vector. The deposition rate for these vapor-deposited glasses was approximately 0.2 nm/s. The glass transition temperature of Alq3 is 450 K.

temperatures during deposition. All measurements were made at room temperature. Each pattern was collected with the incidence angle held above the critical angle of Alq3 and thus represents the bulk structure of the film. In Figure 1, Q_z is the scattering vector out of the plane and Q_{xy} is the scattering vector in the plane. The colors represent scattering intensities from high (dark red) to low (blue). The patterns for the vapor-deposited and the reference spin-coated Alq3 glasses show two scattering features, one at $Q \sim 0.75$ Å^{-1} and another at $Q \sim 1.65$ Å^{-1}. For all of the glasses studied, the scattering feature at

DOI: 10.1021/acs.jpclett.8b03582
J. Phys. Chem. Lett. 2019, 10, 164−170

$Q \sim 1.65$ Å^{-1} is isotropic; this feature roughly corresponds to the nearest neighbor distance for carbons on adjacent Alq3 molecules. For the glasses prepared at T_{sub} = 280 K and T_{sub} = 360 K, the scattering feature at low Q (~0.75 Å^{-1}) is anisotropic. The anisotropic scattering peak occurs at a real space periodicity that is roughly equal to the diameter of an Alq3 molecule; this feature is indicative of a tendency for molecular layering along the surface normal. For the glass deposited at the highest substrate temperature and for the spin-coated glass (which is expected to be similar to a liquid-cooled glass[35]), the low Q (~0.75 Å^{-1}) scattering feature is nearly isotropic. We were not able to deposit films at substrate temperatures above 405 K, presumably due to the high vapor pressure of Alq3. Previous studies have established that Alq3 films vapor-deposited under similar conditions are chemically pure;[36] we further confirmed the purity of the as-deposited film with Raman scattering measurements.

To quantify the tendency for molecular layering, we define an order parameter S_{GIWAXS} as a measure of anisotropy in scattering intensity for values of Q near 0.75 Å^{-1}. A more positive value of S_{GIWAXS} indicates greater localization of scattering intensity along Q_z. Similar order parameters have been described previously;[37,38] however, it is useful to describe the meaning of S_{GIWAXS} in the context of this study. If the order parameter were 1, then all of the scattering intensity would be localized along Q_z; in this case, the "layers" would be parallel to the substrate plane. An S_{GIWAXS} = −0.5 value implies that the "layers" are perpendicular to the substrate plane.

Figure 2 shows two measures of structural anisotropy for Alq3 glasses as a function of substrate temperature during vapor deposition. The S_{GIWAXS} values quantify the tendency for layering to decrease as the substrate temperature increases. The glass prepared at the highest substrate temperature exhibits a negligible tendency for layering, as does the spin-coated glass, which has S_{GIWAXS} = 0.007. The raw sine-corrected scattering intensity, which is often used to qualitatively assess the packing distribution, is shown in Figure S4 for glasses deposited at T_{sub} = 280 and 405 K. Figure 2 also shows ellipsometry measurements indicating that all vapor-deposited glasses of Alq3 exhibit essentially zero birefringence; this is consistent with negligible P_2 order. To our knowledge, this is the first report of a vapor-deposited organic glass that is optically isotropic across a wide range of substrate temperatures. The optical isotropy of Alq3 glasses can be tentatively attributed to its quasi-spheroidal shape (SI Figure 3), and this point is explored below. For comparison, vapor-deposited glasses of three rod-shaped organic semiconductors show birefringence values that range from −0.2 to +0.1.[4] Figure 2 shows very similar X-ray and ellipsometry results for two different film thicknesses, indicating that the glass structure is independent of film thickness.

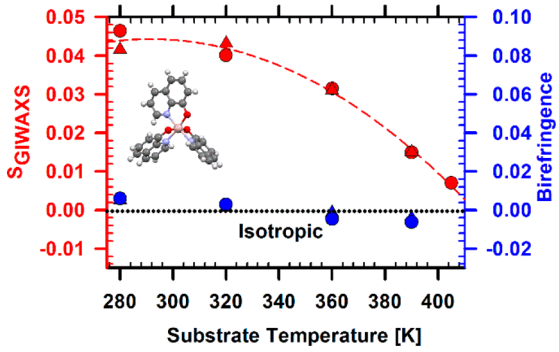

Figure 2. GIWAXS order parameter (red) and the birefringence (blue) of vapor-deposited Alq3 glasses prepared at different substrate temperatures. The GIWAXS order parameter characterizes the structural anisotropy associated with molecular layering; layering is most pronounced at low substrate temperatures. Results for 260 nm (circles) and 540 nm (triangles) films are shown. The dashed red line is a guide to the eye. The dotted black line defines optical and structural isotropy. The deposition rate for these glasses was 0.2 nm/s. The structure of Alq3 is shown as an inset.

Although vapor-deposited Alq3 films have been used as electron transport and emitter layers in OLEDs for over 30 years[39] (from the very inception of OLED technology!), the tendency for molecular layering in Alq3 glasses is reported here for the first time, to the best of our knowledge. Previously, charge transport studies showed that an Alq3 glass prepared at 363 K had an order of magnitude higher DC conductivity than the glass prepared at 303 K.[40] The changes in molecular packing shown in Figure 2 could shed new light on the interpretation of these charge transport measurements.

We also observe that the substrate temperature during deposition influences the periodicity associated with the layering feature in vapor-deposited Alq3 glasses. To evaluate how the changes in layer spacing relate to the surface equilibration mechanism, Figure 3 shows the position of the anisotropic peak along Q_z over a range of substrate temperatures for two different deposition rates. To a reasonable approximation, lowering the deposition rate by a factor of 7 has the same impact on the peak position as increasing the substrate temperature by 10 K (a similar observation can be made for the S_{GIWAXS} order parameter, as shown in Figure S5). This supports the surface equilibration mechanism, as (1) both lowering the deposition rate and raising the substrate temperature should allow the molecules to more closely approach equilibrium before they are trapped by further deposition and (2) the observed temperature dependence of ~12 K/decade is much weaker than that expected for bulk molecular mobility near T_g, consistent with the idea that surface mobility[41] controls the structure of PVD glasses. For the comparison shown in Figure 3, we chose to focus on the peak position along Q_z, as most of the scattering intensity is

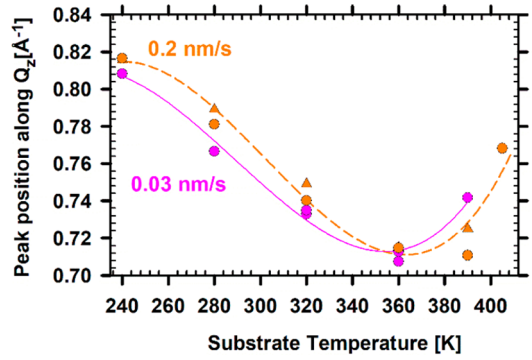

Figure 3. Peak position along Q_z obtained from GIWAXS as a function of substrate temperature for Alq3 glasses prepared at two deposition rates: 0.2 nm/s (orange) and 0.03 nm/s (pink). Consistent with the surface equilibration mechanism, slower deposition and higher substrate temperature have similar effects on bulk glass structure. Results for 260−280 nm (circles) and 540 nm (triangles) films are shown. The lines are guides to the eye.

DOI: 10.1021/acs.jpclett.8b03582
J. Phys. Chem. Lett. 2019, 10, 164−170

localized along Q_z. We note that differences in the peak position along Q_z, between glasses prepared at different substrate temperatures, cannot be directly interpreted as a change in glass density. The peak position along Q_{xy} also varies as a function of substrate temperature, exhibiting the opposite trend (Figure S2). Previous studies by Yokoyama et al.[35] have established that the density of Alq3 glasses varies less than 2% with preparation conditions, as opposed to the 10% variation in peak position shown in Figure 3.

To test if the observed structural anisotropy of vapor-deposited Alq3 glasses can be understood in terms of structures preferred at the surface of the equilibrium liquid, we performed atomistic molecular dynamics simulations of the supercooled liquid of Alq3 at 470, 490, and 550 K. For this model,[42] it has been previously reported that T_g = 455 K at simulation cooling rates. The equilibrium liquid of Alq3 exhibits a temperature-dependent tendency for layering at the free surface (shown in Figure 4A) similar to what is seen

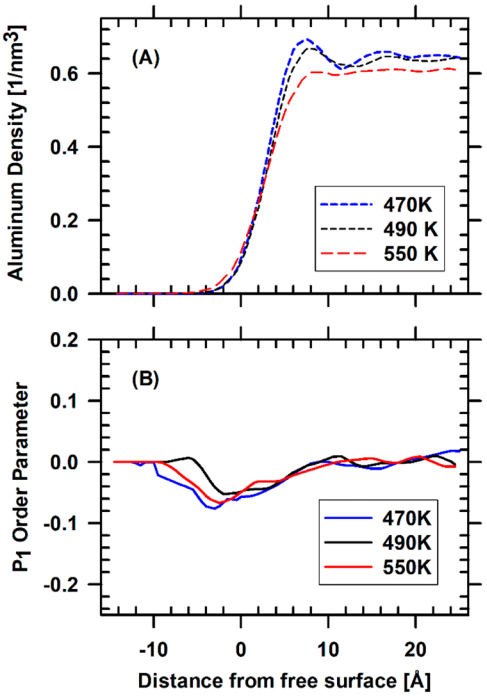

Figure 4. Structural features of the free surface of supercooled Alq3 liquid as obtained by molecular dynamics simulations. (A) Aluminum density plotted as a function of depth, showing oscillations that are responsible for layering in PVD glasses. (B) The P_1 order parameter for the dipole moment vector of Alq3 as a function of depth in the film, showing polar order that is trapped during deposition to produce large surface potentials. For both panels, the free surface is defined by position, where the Alq3 density is equal to half of the bulk value.

experimentally in X-ray reflectivity studies of metallic liquids,[34,43] in dielectric liquids,[44] and in the isotropic phase of liquid crystal formers.[45] At a temperature of 470 K, the spacing between the two peaks in the density profile is roughly ~9 Å. Experimentally, the length scale of the layering feature ($2\pi/Q_z$) seen in vapor-deposited glasses is ~7.5−9.0 Å. As we explain below, this result is consistent with the hypothesis that the bulk structure of vapor-deposited glasses is inherited from the surface structure of the equilibrium liquid.

The simulated supercooled liquid of Alq3 also exhibits surface dipole orientation, a feature that has been observed experimentally for several molecular liquids, and is known to persist even far above T_g.[46] In Figure 4B, the P_1 order parameter $\langle \cos\theta \rangle$ is shown for the classical dipole moment vector of Alq3 relative to the surface normal. The negative value of the order parameter indicates that the positive end of the Alq3 dipole has a tendency to point toward the vacuum at the surface of the equilibrium liquid. Experimentally a positive surface potential in vapor-deposited Alq3 glasses has been reported[29,47] which implies that there is a bulk orientation of the dipole moment vector such that the positive ends on average point toward the vacuum interface. Figure 4B is consistent with the surface equilibration mechanism which implies a close similarity between the bulk structure of the PVD glass and the surface structure of the equilibrium liquid. The surface potential reported for PVD glasses of Alq3 is about 1% of the value that would be obtained if the dipole vector of every Alq3 molecule pointed exactly toward the vacuum interface, while in simulations the maximum orientation seen at the free surface of the supercooled liquid at 470 K is 6% (evaluated at the point where the density is half the bulk liquid density). The dipole orientation at the equilibrium free surface is likely an upper bound to what can be trapped into the bulk glass, with the latter depending upon substrate temperature and deposition rate.

The molecular simulations can also be used to understand the extremely small birefringence observed in vapor-deposited Alq3 glasses (Figure 2). The eigenvector associated with the largest eigenvalue of the polarizability tensor of Alq3 shows a very small P_2 ordering (−0.02) at the free surface of the simulated equilibrium liquid (Figure S1). This small P_2 ordering when combined with the small anisotropy of the Alq3 polarizability tensor (Table S1) is consistent with the observed lack of birefringence. (Both the low level of P_2 order and the nearly isotropic polarizability tensor are consistent with the quasi-spheroidal shape of Alq3.) Thus, the surface equilibration mechanism, in combination with the simulation results, can successfully explain the optical isotropy, tendency toward layering, and P_1 order in PVD glasses of Alq3.

The surface equilibration mechanism can also be used to rationalize the dependence of structural anisotropy on substrate temperature (Figure 2) in Alq3 glasses by invoking the experimental observation that the mobile surface layer in organic glasses grows in thickness with increasing temperature.[48] Previous simulations of the vapor deposition process have established that the structure that gets locked into the glass is determined by the thickness of the mobile surface layer,[4] which in turn is dependent on the substrate temperature during deposition. At lower substrate temperatures, as the mobile layer is only one monolayer thick, the structure from only the top monolayer of the liquid gets locked into the glass. At the top monolayer of the simulated supercooled Alq3 liquid, the tendency for layering is strong, and hence, glasses prepared at lower substrate temperatures exhibit a strong tendency for bulk molecular layering. At higher substrate temperature, the structure from the second or third layer of the liquid gets locked into the glass, as the mobile layer is thicker. Since the tendency for layering is significantly reduced in the second monolayer and negligible in subsequent layers, this results in less structural anisotropy being trapped into the bulk glass.

Recent years have seen considerable progress in modeling the process of vapor deposition. Wenzel and co-workers performed force-field-based Monte Carlo simulations to simulate spontaneous polarization in vapor-deposited glasses;

DOI: 10.1021/acs.jpclett.8b03582
J. Phys. Chem. Lett. 2019, 10, 164−170

their simulations utilize ideas that overlap with the surface equilibration mechanism. For example, enhanced surface mobility is mimicked in their simulations by utilizing simulated annealing to equilibrate surface molecules at temperatures much higher than that of the "already deposited and fixed molecules". These simulations semiquantitatively reproduce the surface potential trends observed for glasses vapor-deposited onto room temperature substrates.[49] Han et al. simulated the vapor deposition process for a number of OLED molecules; their simulations reproduce the trend in P_2 order as a function of substrate temperature observed experimentally.[50] In these simulations, the "last deposited molecule" is held at a higher temperature than the bulk film, thus introducing surface mobility. As noted in the introduction, Lyubimov et al.[51] showed that the P_2 order near the surface of the supercooled liquids of several OLED molecules could account for the P_2 order trapped into the glasses vapor-deposited at various substrate temperatures and rates.

While previous models of structure in PVD glasses have concentrated on understanding P_1 and P_2 order, we show that the surface equilibration mechanism simultaneously accounts for several different structural features of a model vapor-deposited glass. This is the first study to provide a microscopic explanation for the origin of the commonly observed anisotropic scattering feature associated with molecular layering.[9,37,52] Both the molecular layering features and P_1 order in Alq3 are shown to originate from the surface structure of the equilibrium supercooled liquid. On the basis of simulations, this approach predicts a spacing between Alq3 molecules in the glass which is consistent with experimental findings. In agreement with the surface equilibration mechanism, the structure of PVD glasses of Alq3 is found to depend on a combination of deposition rate and substrate temperature consistent with facilitation by surface mobility. In addition, the surface equilibration mechanism accounts for the existence of polar order in vapor-deposited Alq3 glasses, correctly predicting a positive polarization.

Broad anisotropic scattering peaks and P_1 order are common features of vapor-deposited glasses,[9,25,26,30] and we expect that the surface equilibration mechanism generally provides an explanation for these features. By connecting the phenomenon in vapor-deposited glasses to structure at the free surface of the equilibrium liquid, we bridge the relatively new field of vapor-deposited glasses to decades of research on the structure of liquid surfaces. There is also a practical aspect to this new understanding. Full scale simulations of vapor-deposited glasses are limited by the short time scales available in simulations. The surface structure of the liquid on the other hand can be reliably simulated and is also accessible by experiments. By providing an understanding of nonequilibrium structural features on the basis of equilibrium surface structure, this work significantly advances our ability to design anisotropic glassy solids. Thus, we anticipate that computer simulations of the surface of equilibrium liquids can succeed in identifying molecules that promote packing motifs in vapor-deposited glasses that are desirable for organic electronic devices.

METHODS

Sample Preparation. Alq3 (99.995% purity) purchased from Sigma-Aldrich was vapor-deposited without further purification onto a ⟨100⟩ silicon wafer with 2 nm of native oxide in a vacuum chamber with a base pressure of ~10^{-6} Torr. Samples were prepared either at deposition rates near 0.2 nm/s (0.14−0.23 nm/s) or near 0.03 nm/s (0.02−0.04 nm/s). For the spin-coated sample, Alq3 was dissolved in chloroform at a concentration of 15 mg/mL. The spinning speed was 1500 rpm, and the time was 50 s. This procedure was described by Yokoyama.[35]

GIWAXS. Grazing incidence X-ray scattering measurements were performed at the Stanford Synchrotron Radiation Lightsource in beamline 11-3 which has a wavelength of 0.973 Å. The sample to detector distance was calibrated with LaB_6. The data reported was acquired with an incidence angle of 0.14°, which is appropriate for studying the bulk structure of vapor-deposited Alq3 glasses.[37] For a few samples, we verified that very similar values of S_{GIWAXS} were obtained from measurements performed at 0.16°, as expected.

To evaluate the S_{GIWAXS} order parameter, we utilize the dependence of the scattering intensity upon the azimuthal angle χ; χ is 0° along Q_z and 90° along Q_{xy}. For χ values from 10 to 85°, we integrated the data in a Q range from 0.5 to 1.2 $Å^{-1}$. The data in the missing wedge of the pattern (near χ = 0°) was obtained by extrapolation of the data at larger χ. S_{GIWAXS} was then calculated using the equation

$$S_{GIWAXS} = \frac{1}{2}(3\langle\cos^2\chi\rangle - 1) \tag{1}$$

with $\langle\cos^2\chi\rangle$ evaluated as follows:

$$\langle\cos^2\chi\rangle = \frac{\int_0^{90} I(\chi)(\cos^2\chi)(\sin\chi)\,d\chi}{\int_0^{90} I(\chi)(\sin\chi)\,d\chi} \tag{2}$$

For the data in Figure 3, the peak positions along Q_z were obtained by averaging data with χ between 10 and 15°.

Spectroscopic Ellipsometry. Data was collected at the three angles (50, 60, and 70°). The birefringence was obtained by fitting data in the wavelength range of 500−1000 nm with a uniaxial Cauchy model. The birefringence was evaluated at a wavelength of 632.8 nm.

Simulation Methods. Atomistic simulations of the *mer*-isomer of Alq3 were performed with the OPLS-style force field of Lukyanov et al.[42,53] and the LAMMPS simulation package. Lennard-Jones and electrostatic interactions employed a cutoff of 1.22 nm with the PPPM method (mean error = 10^{-5}) to account for long-range electrostatics. A time step of 2.5 fs was used for the velocity-Verlet integrator with the RATTLE algorithm to constrain C−H bond lengths. A free surface was prepared by slowly stretching a 500-molecule bulk Alq3 simulation until a gap appeared between the top and bottom surfaces. The distances between the top and bottom surfaces were 20 nm for all simulation temperatures, ensuring negligible interactions between opposing surfaces. Simulations of these thin films were equilibrated for a total of 50 ns at 470, 490, and 550 K. Sampling of the surface structure following equilibration occurred at 0.25 ns intervals for a total of 150 ns. Mass density and aluminum density profiles were computed and averaged over all configurations. These configurations were also used to compute the P_1 and P_2 order parameters. The P_1 order parameter was calculated using the classical dipole moment unit vector of each Alq3 molecule and the surface normal $\mathbf{n}_z$:

$$P_1 = \langle\mathbf{n}\cdot\mathbf{n}_z\rangle = \langle\cos(\alpha)\rangle \tag{3}$$

DOI: 10.1021/acs.jpclett.8b03582
J. Phys. Chem. Lett. 2019, 10, 164−170

For the P_2 order parameter calculations, a unit vector in the direction of the eigenvector associated with the largest eigenvalue of the dipole polarizability tensor determined via B3LYP/6-31G** was used:

$$P_2 = \langle \mathbf{P_2}(\mathbf{n}\cdot\mathbf{n_z})\rangle = \frac{3}{2}\langle \cos^2(\alpha)\rangle - \frac{1}{2} \quad (4)$$

For all quantities, the results shown in Figure 4 are averaged over both the top and bottom surfaces within the simulation box.

■ ASSOCIATED CONTENT

Supporting Information

The Supporting Information is available free of charge on the ACS Publications website at DOI: 10.1021/acs.jpclett.8b03582.

Calculated polarizability tensor of Alq3 (Table S1), calculated P_2 order parameter at the free surface of the equilibrium Alq3 liquid (Figure S1), experimental X-ray scattering peak positions along Q_{xy} (Figure S2), calculated dipole moment vector direction in the Alq3 molecule (Figure S3), experimental sine-corrected X-ray intensity curves (Figure S4), and the experimental S_{GIWAXS} order parameter for a slower deposition rate (Figure S5) (PDF)

■ AUTHOR INFORMATION

Corresponding Author

*Phone: 608-262-7273. E-mail: ediger@chem.wisc.edu.

ORCID

Kushal Bagchi: 0000-0002-9145-554X
Nicholas E. Jackson: 0000-0002-1470-1903
Ankit Gujral: 0000-0002-5065-2694
Chengbin Huang: 0000-0002-0759-0942
Michael F. Toney: 0000-0002-7513-1166
Juan J. de Pablo: 0000-0002-3526-516X
M. D. Ediger: 0000-0003-4715-8473

Notes

The authors declare no competing financial interest.

■ ACKNOWLEDGMENTS

The experimental work was supported by the US Department of Energy, Office of Basic Energy Sciences, Division of Materials Sciences and Engineering, Award DE-SC0002161. The authors gratefully acknowledge use of facilities and instrumentation supported by NSF through the University of Wisconsin Materials Research Science and Engineering Center (DMR-1720415). N.E.J. acknowledges support from the Argonne National Laboratory Maria Goeppert Mayer Named Fellowship. We acknowledge the computing resources provided on Blues and Bebop, the high-performance computing clusters operated by the Laboratory Computing Resource Center at Argonne National Laboratory. Use of the Stanford Synchrotron Radiation Lightsource, SLAC National Accelerator Laboratory, is supported by the U.S. Department of Energy, Office of Science, Office of Basic Energy Sciences, under Contract DE-AC02-76SF00515. We thank David Field for helpful discussions.

■ REFERENCES

(1) Yokoyama, D. Molecular Orientation in Small-Molecule Organic Light-Emitting Diodes. *J. Mater. Chem.* **2011**, *21*, 19187.
(2) Ràfols-ribé, J.; Will, P.; Hänisch, C.; Gonzalez-silveira, M.; Lenk, S.; Rodríguez-viejo, J.; Reineke, S. High-Performance Organic Light-Emitting Diodes Comprising Ultrastable Glass Layers. *Sci. Adv.* **2018**, *4*, eaar8332.
(3) Ishii, K.; Nakayama, H. Structural Relaxation of Vapor-Deposited Molecular Glasses and Supercooled Liquids. *Phys. Chem. Chem. Phys.* **2014**, *16*, 12073−12092.
(4) Dalal, S. S.; Walters, D. M.; Lyubimov, I.; de Pablo, J. J.; Ediger, M. D. Tunable Molecular Orientation and Elevated Thermal Stability of Vapor-Deposited Organic Semiconductors. *Proc. Natl. Acad. Sci. U. S. A.* **2015**, *112*, 4227−4232.
(5) Ramos, S. L. L. M.; Oguni, M.; Ishii, K.; Nakayama, H. Character of Devitrification, Viewed from Enthalpic Paths of the Vapor-Deposited Ethylbenzene Glasses. *J. Phys. Chem. B* **2011**, *115*, 14327−14332.
(6) Debenedetti, P. G.; Stillinger, F. H. Supercooled Liquids and the Glass Transition. *Nature* **2001**, *410*, 259.
(7) Angell, A. Thermodynamics: Liquid Landscape. *Nature* **1998**, *393*, 521.
(8) Yu, H. B.; Tylinski, M.; Ediger, M. D.; Richert, R. Suppression of β Relaxation in Vapor-Deposited Ultrastable Glasses. *Phys. Rev. Lett.* **2015**, *115*, 185501.
(9) Pérez-castañeda, T.; Rodríguez-tinoco, C.; Rodríguez-viejo, J.; Ramos, M. A. Suppression of Tunneling Two-Level Systems in Ultrastable Glasses of Indomethacin. *Proc. Natl. Acad. Sci. U. S. A.* **2014**, *111*, 11275−11280.
(10) Qiu, Y.; Antony, L. W.; de Pablo, J. J.; Ediger, M. D. Photostability Can Be Significantly Modulated by Molecular Packing in Glasses. *J. Am. Chem. Soc.* **2016**, *138*, 11282−11289.
(11) Dawson, K. J.; Kearns, K. L.; Ediger, M. D.; Sacchetti, M. J.; Zografi, G. D. Highly Stable Indomethacin Glasses Resist Uptake of Water Vapor. *J. Phys. Chem. B* **2009**, *113*, 2422−2427.
(12) Esaki, Y.; Komino, T.; Matsushima, T.; Adachi, C. Enhanced Electrical Properties and Air Stability of Amorphous Organic Thin Films by Engineering Film Density. *J. Phys. Chem. Lett.* **2017**, *8*, 5891−5897.
(13) Brian, C. W.; Yu, L. Surface Self-Diffusion of Organic Glasses. *J. Phys. Chem. A* **2013**, *117*, 13303−13309.
(14) Stevenson, J. D.; Wolynes, P. G. On the Surface of Glasses. *J. Chem. Phys.* **2008**, *129*, 234514.
(15) Lin, H.; Lin, C.; Chang, H.; Lin, Y.; Wu, C.; Chen, Y.; Chen, R.; Chien, Y. .; Wong, K. T. Anisotropic Optical Properties and Molecular Orientation in Vacuum-Deposited ter(9,9-Diarylfluorene)s Thin Films Using Spectroscopic Ellipsometry. *J. Appl. Phys.* **2004**, *95*, 881−886.
(16) Hellman, F. Surface-Induced Ordering: A Model for Vapor-Deposition Growth of Amorphous Materials. *Appl. Phys. Lett.* **1994**, *64*, 1947−1949.
(17) Yokoyama, D.; Setoguchi, Y.; Sakaguchi, A.; Suzuki, M.; Adachi, C. Orientation Control of Linear-Shaped Molecules in Vacuum-Deposited Organic Amorphous Films and Its Effect on Carrier Mobilities. *Adv. Funct. Mater.* **2010**, *20*, 386−391.
(18) Xing, X.; Zhong, L.; Zhang, L.; Chen, Z.; Qu, B.; Chen, E.; Xiao, L. Essential Differences of Organic Films at the Molecular Level via Vacuum Deposition and Solution Processes for Organic Light-Emitting Diodes. *J. Phys. Chem. C* **2013**, *117*, 25405−25408.
(19) Schmidt, T. D.; Lampe, T.; R, D. S. M.; Djurovich, P. I.; Thompson, M. E.; Brütting, W. Emitter Orientation as a Key Parameter in Organic Light-Emitting Diodes. *Phys. Rev. Appl.* **2017**, *8*, 37001.
(20) Frischeisen, J.; Yokoyama, D.; Endo, A.; Adachi, C.; Brütting, W. Increased Light Outcoupling Efficiency in Dye-Doped Small Molecule Organic Light-Emitting Diodes with Horizontally Oriented Emitters. *Org. Electron.* **2011**, *12*, 809−817.
(21) Sakai, Y.; Shibata, M.; Yokoyama, D. Simple Model-Free Estimation of Orientation Order Parameters of Vacuum-Deposited

DOI: 10.1021/acs.jpclett.8b03582
J. Phys. Chem. Lett. 2019, 10, 164−170

and Spin-Coated Amorphous Films Used in Organic Light-Emitting Diodes. *Appl. Phys. Express* **2015**, *8*, 096601.
(22) Gurau, M. C.; Delongchamp, D. M.; Vogel, B. M.; Lin, E. K.; Fischer, D. A.; Sambasivan, S.; Richter, L. J. Measuring Molecular Order in Poly (3-Alkylthiophene) Thin Films with Polarizing Spectroscopies. *Langmuir* **2007**, *23*, 834−842.
(23) Delongchamp, D. M.; Kline, R. J.; Fischer, D. A.; Richter, L. J.; Toney, M. F. Molecular Characterization of Organic Electronic Films. *Adv. Mater.* **2011**, *23*, 319−337.
(24) Walters, D. M.; Antony, L.; de Pablo, J. J.; Ediger, M. D. Influence of Molecular Shape on the Thermal Stability and Molecular Orientation of Vapor-Deposited Organic Semiconductors. *J. Phys. Chem. Lett.* **2017**, *8*, 3380−3386.
(25) Rodríguez-Tinoco, C.; Gonzalez-Silveira, M.; Ràfols-Ribé, J.; Garcia, G.; Rodríguez-Viejo, J. Highly Stable Glasses of Celecoxib: Influence on Thermo-Kinetic Properties, Microstructure and Response towards Crystal Growth. *J. Non-Cryst. Solids* **2015**, *407*, 256−261.
(26) Dawson, K. J.; Zhu, L.; Yu, L.; Ediger, M. D. Anisotropic Structure and Transformation Kinetics of Vapor-Deposited Indomethacin Glasses. *J. Phys. Chem. B* **2011**, *115*, 455−463.
(27) Singh, S.; De Pablo, J. J. A Molecular View of Vapor Deposited Glasses. *J. Chem. Phys.* **2011**, *134*, 194903.
(28) Noriega, R.; Rivnay, J.; Vandewal, K.; Koch, F. P. V.; Stingelin, N.; Smith, P.; Toney, M. F.; Salleo, A. A General Relationship between Disorder, Aggregation and Charge Transport in Conjugated Polymers. *Nat. Mater.* **2013**, *12*, 1038.
(29) Noguchi, Y.; Miyazaki, Y.; Tanaka, Y.; Sato, N.; Nakayama, Y.; Schmidt, T. D.; Brütting, W.; Ishii, H. Charge Accumulation at Organic Semiconductor Interfaces due to a Permanent Dipole Moment and Its Orientational Order in Bilayer Devices. *J. Appl. Phys.* **2012**, *111*, 114508.
(30) Osada, K.; Goushi, K.; Kaji, H.; Adachi, C.; Ishii, H.; Noguchi, Y. Observation of Spontaneous Orientation Polarization in Evaporated Films of Organic Light-Emitting Diode Materials. *Org. Electron.* **2018**, *58*, 313−317.
(31) Noguchi, Y.; Lim, H.; Isoshima, T.; Ito, E.; Hara, M. Influence of the Direction of Spontaneous Orientation Polarization on the Charge Injection Properties of Organic Light-Emitting Diodes. *Appl. Phys. Lett.* **2013**, *102*, 203306.
(32) Murawski, C.; Elschner, C.; Lenk, S.; Reineke, S.; Gather, M. C. Investigating the Molecular Orientation of Ir(ppy)3 and Ir(ppy)2-(acac) Emitter Complexes by X-Ray Diffraction. *Org. Electron.* **2018**, *53*, 198−204.
(33) Liu, T.; Exarhos, A. L.; Alguire, E. C.; Gao, F.; Salami-Ranjbaran, E.; Cheng, K.; Jia, T.; Subotnik, J. E.; Walsh, P. J.; Kikkawa, J. M.; et al. Birefringent Stable Glass with Predominantly Isotropic Molecular Orientation. *Phys. Rev. Lett.* **2017**, *119*, 95502.
(34) Regan, M. J.; Kawamoto, E. H.; Lee, S.; Pershan, P. S.; Maskil, N.; Deutsch, M.; Magnussen, O.; Ocko, B.; Berman, L. Surface Layering in Liquid Gallium: An X-Ray Reflectivity Study. *Phys. Rev. Lett.* **1995**, *75*, 2498.
(35) Shibata, M.; Sakai, Y.; Yokoyama, D. Advantages and Disadvantages of Vacuum-Deposited and Spin-Coated Amorphous Organic Semiconductor Films for Organic Light-Emitting Diodes. *J. Mater. Chem. C* **2015**, *3*, 11178−11191.
(36) Jian, Z. A.; Luo, Y. Z.; Chung, J. M.; Tang, S. J.; Kuo, M. C.; Shen, J. L.; Chiu, K. C.; Yang, C. S.; Chou, W. C.; Dai, C. F.; et al. Effects of Isomeric Transformation on Characteristics of Alq3 Amorphous Layers Prepared by Vacuum Deposition at Various Substrate Temperatures. *J. Appl. Phys.* **2007**, *101*, 123708.
(37) Gujral, A.; O'Hara, K. A.; Toney, M. F.; Chabinyc, M. L.; Ediger, M. D. Structural Characterization of Vapor-Deposited Glasses of an Organic Hole Transport Material with X-Ray Scattering. *Chem. Mater.* **2015**, *27*, 3341−3348.
(38) Hammond, M. R.; Kline, R. J.; Herzing, A. A.; Richter, L. J.; Germack, D. S.; Ro, H.; Soles, C. L.; Fischer, D. A.; Xu, T.; Yu, L.; et al. Molecular Order in High-Efficiency Polymer/Fullerene Bulk Heterojunction Solar Cells. *ACS Nano* **2011**, *5*, 8248−8257.
(39) Tang, C. W.; VanSlyke, S. A. Organic Electroluminescent Diodes. *Appl. Phys. Lett.* **1987**, *51*, 913−915.
(40) Chung, J. M.; Luo, Y. Z.; Jian, Z. A.; Kuo, M. C.; Yang, C. S.; Chou, W. C.; Chiu, K. C. Effects of Substrate Temperature on the Properties of Alq3 Amorphous Layers Prepared by Vacuum Deposition. *Jpn. J. Appl. Phys.* **2004**, *43*, 1631.
(41) Ruan, S.; Zhang, W.; Sun, Y.; Ediger, M. D.; Yu, L. Surface Diffusion and Surface Crystal Growth of Tris-Naphthyl Benzene Glasses. *J. Chem. Phys.* **2016**, *145*, 064503.
(42) Lukyanov, A.; Lennartz, C.; Andrienko, D. Amorphous Films of tris(8-Hydroxyquinolinato)aluminium: Force-Field, Morphology, and Charge Transport. *Phys. Status Solidi A* **2009**, *12*, 2737−2742.
(43) D'Evelyn, M.; Rice, S. A. Structure in the Density Profile at the Liquid-Metal-Vapor Interface. *Phys. Rev. Lett.* **1981**, *47*, 1844.
(44) Chattopadhyay, S.; Uysal, A.; Stripe, B.; Ehrlich, S.; Karapetrova, E. A.; Dutta, P. Surface Order in Cold Liquids : X-Ray Reflectivity Studies of Dielectric Liquids and Comparison to Liquid Metals. *Phys. Rev. B: Condens. Matter Mater. Phys.* **2010**, *81*, 184206.
(45) Ocko, B. M.; Braslau, A.; Pershan, P. S.; Als-Nielsen, J.; Deutsch, M. Quantized Layer Growth at Liquid-Crystal Surfaces. *Phys. Rev. Lett.* **1986**, *57*, 94−97.
(46) Stanners, C. D.; Du, Q.; Chin, R. P.; Somorjai, G. A.; Shen, Y. Polar Ordering at the Liquid-Vapor Interface of N-Alcohols (C1-C8). *Chem. Phys. Lett.* **1995**, *232*, 407−413.
(47) Ito, E.; Washizu, Y.; Hayashi, N.; Ishii, H.; Matsuie, N.; Tsuboi, K.; Ouchi, Y.; Yamashita, K.; Seki, K. Spontaneous Buildup of Giant Surface Potential by Vacuum Deposition of Alq3 and Its Removal by Visible Light Irradiation. *J. Appl. Phys.* **2002**, *92*, 7306−7310.
(48) Swallen, S. F.; Kearns, K. L.; Mapes, M. K.; Kim, Y. S.; McMahon, R. J.; Ediger, M. D.; Wu, T.; Yu, L.; Satija, S. Organic Glasses with Exceptional Thermodynamic and Kinetic Stability. *Science* **2007**, *315*, 353−356.
(49) Friederich, P.; Rodin, V.; Von Wrochem, F.; Wenzel, W. Built-in Potentials Induced by Molecular Order in Amorphous Organic Thin Films. *ACS Appl. Mater. Interfaces* **2018**, *10*, 1881−1887.
(50) Youn, Y.; Yoo, D.; Song, H.; Kang, Y.; Kim, K. Y.; Jeon, S. H.; Cho, Y.; Chae, K.; Han, S. All-Atom Simulation of Molecular Orientation in Vapor-Deposited Organic Light-Emitting Diodes. *J. Mater. Chem. C* **2018**, *6*, 1015−1022.
(51) Lyubimov, I.; Antony, L.; Walters, D. M.; Rodney, D.; Ediger, M. D.; de Pablo, J. J. Orientational Anisotropy in Simulated Vapor-Deposited Molecular Glasses. *J. Chem. Phys.* **2015**, *143*, 094502.
(52) Gujral, A.; Gómez, J.; Jiang, J.; Huang, C.; O'Hara, K. A.; Toney, M. F.; Chabinyc, M. L.; Yu, L.; Ediger, M. D. Highly Organized Smectic-like Packing in Vapor-Deposited Glasses of a Liquid Crystal. *Chem. Mater.* **2017**, *29*, 849−858.
(53) Rühle, V.; Lukyanov, A.; May, F.; Schrader, M.; Veho, T.; Kirkpatrick, J.; Andrienko, D. Microscopic Simulations of Charge Transport in Disordered Organic Semiconductors. *J. Chem. Theory Comput.* **2011**, *7*, 3335−3345.

DOI: 10.1021/acs.jpclett.8b03582
J. Phys. Chem. Lett. 2019, 10, 164−170